


Article

1D–3D Coupling Algorithm of Gas Flow for the Valve System in a Compression Ignition Engine

Kyeong-Ju Kong 

Training Ship Management Center, Pukyong National University, Busan 48513, Korea; kjkong@pknu.ac.kr;
Tel.: +82-51-629-6186

Abstract: Emission control devices such as selective catalytic reduction (SCR), exhaust gas recirculation (EGR), and scrubbers were installed in the compression ignition (CI) engine, and flow analysis of intake air and exhaust gas was required to predict the performance of the CI engine and emission control devices. In order to analyze such gas flow, it was inefficient to comprehensively analyze the engine's cylinder and intake/exhaust systems because it takes a lot of computation time. Therefore, there is a need for a method that can quickly calculate the gas flow of the CI engine in order to shorten the development process of emission control devices. It can be efficient and quickly calculated if only the parts that require detailed observation among the intake/exhaust gas flow of the CI engine are analyzed in a 3D approach and the rest are analyzed in a 1D approach. In this study, an algorithm for gas flow analysis was developed by coupling 1D and 3D in the valve systems and comparing with experimental results for validation. Analyzing the intake/exhaust gas flow of the CI engine in a 3D approach took about 7 days for computation, but using the developed 1D–3D coupling algorithm, it could be computed within 30 min. Compared with the experimental results, the exhaust pipe pressure occurred an error within 1.80%, confirming the accuracy and it was possible to observe the detailed flow by showing the contour results for the part analyzed in the 3D zone. As a result, it was possible to accurately and quickly calculate the gas flow of the CI engine using the 1D–3D coupling algorithm applied to the valve system, and it was expected that it can be used to shorten the process for analyzing emission control devices, including predicting the performance of the CI engine.

Keywords: 1D–3D coupling; coupling algorithm; valve system; gas flow analysis; CI engine



Citation: Kong, K.-J. 1D–3D Coupling Algorithm of Gas Flow for the Valve System in a Compression Ignition Engine. *J. Mar. Sci. Eng.* **2021**, *9*, 1061. <https://doi.org/10.3390/jmse9101061>

Academic Editor:
Evangelos Keramaris

Received: 11 September 2021
Accepted: 24 September 2021
Published: 27 September 2021

Publisher's Note: MDPI stays neutral with regard to jurisdictional claims in published maps and institutional affiliations.



Copyright: © 2021 by the author. Licensee MDPI, Basel, Switzerland. This article is an open access article distributed under the terms and conditions of the Creative Commons Attribution (CC BY) license (<https://creativecommons.org/licenses/by/4.0/>).

1. Introduction

Environmental pollutants emitted from compression ignition (CI) engines used for propulsion and electricity generation of ships were regulated according to the regulations of the International Maritime Organization (IMO) and regulations on SO_x and NO_x are gradually being strengthened. According to the IMO MARPOL 73/78 Annex VI, from 2020, the sulfur content of fuel oil used by all ships on international voyages was regulated to 0.5% (m/m, mass by mass) or less [1]. The low-sulfur fuel oil was used or the scrubbers were installed to respond to sulfur content regulations [2], and the number of ships using liquefied natural gas (LNG) as fuel is increasing [3]. In particular, ships sailing on the emission control areas (ECAs) must use fuel oil with a sulfur content of 0.1% (m/m) or less, and due to this sulfur content regulation, it is inevitable for ship owners to increase their operating costs [4]. Therefore, ship owners are operating ships by comparing the cost aspect of using the low-sulfur fuel oil and installing a scrubber [5]. In addition, when the low sulfur fuel oil was used, excessive wear may occur on the fuel system components such as the plunger and barrel of the fuel injection pump, and it can cause serious problems in the lubrication system, such as temperature rise of the cylinder liner and piston ring, oxidation of cylinder oil, promotion of oil film breakage, and deterioration of the piston ring motion [6].

Tier III related to NO_x emissions has been in effect since 2016, and the NO_x emission allowance was determined according to the engine speed [7]. In order to meet the NO_x

emission regulation, the method of installing the exhaust gas recirculation (EGR) or the selective catalytic reduction (SCR) on an existing engine or using a dual fuel engine is being used [8]. EGR suppresses NO_x generation by circulating the exhaust gas to decrease the exhaust gas temperature and oxygen concentration. However, since a separate cooling device is required to lower the combustion temperature, space is limited in order to be installed in an existing ship, and there is a disadvantage of reducing the output and efficiency of the engine [9]. SCR is a technology that reduces NO_x contained in the exhaust gas to N_2 and H_2O and uses a reducing agent such as urea [10]. In order to apply the EGR and SCR for reducing NO_x to the exhaust system of the CI engine, it should be installed with consideration of the interaction with the gas flow of the intake/exhaust systems [11].

Exhaust emissions and the engine performance vary with combustion, and there are study results showing that partially premixed combustion (PPC) can obtain a higher effective expansion ratio than conventional diesel combustion (CDC) because it enables a faster combustion event [12]. Consequently, PPC is proposed as promising for high indicated efficiency and low exhaust emissions in terms of NO_x and Soot. Another factor that affects the engine efficiency and emissions is the fuel injection system. As a result of analyzing the effects of multi-hole nozzles (MHN) and hollow cone nozzle (HCN) according to the injector concept, the combination of the HCN injectors and conventional combustion architectures performed worse in terms of emissions and efficiencies [13]. In addition, a method of using a CFD simulation tool to find an optimized configuration for various piston bowl shapes has been proposed, and methods using CFD have been proposed as a method to study the effect of a shape change of a component on an engine.

Advanced studies using computational fluid dynamics (CFD) are being conducted to analyze emission control devices installed in the CI engines. Chowdary et al. analyzed the performance of a single-cylinder CI engine and reduction of emission using EGR using 3D CFD and suggested a method to reduce NO_x and soot by adjusting the fuel injection timing [14]. Zhu et al. performed simulation analysis on the high-pressure SCR system in a marine diesel using the commercial CFD code Ansys Fluent and analyzed the characteristics of vaporizer/mixers [15]. These advanced studies are focused on analyzing the emission control device, and if the engine specifications change, the characteristics will also change. In order to design a marine CI engine, it is necessary to analyze not only the CI engine but also the entire system including the emission control device.

The 3D gas flow analysis using commercial CFD codes is used for engine performance prediction and design. Robbio et al. analyzed the effect of the engine speed on combustion in a dual fuel engine using a CFD approach [16]. However, the 3D approach CFD has the disadvantage that it takes a long time to compute, so it is not suitable for analyzing the intake/exhaust gas flow by applying the emission control devices installed in the CI engine.

Analyzing gas flow with a 1D approach has disadvantages in that it is not accurate in complex shapes and cannot be used for intuitive analysis because the calculation results cannot be expressed as contours. For this reason, an approach that couples 1D and 3D is being used to analyze the gas flow in the CI engine. Liu et al. analyzed the effect of cylinder deactivation on fuel saving and emission by coupling the 1D model and the 3D combustion model and verified the accuracy by comparing the experiment and the results [17]. Wurzenberger simulated SCR by coupling 1D and 3D approaches and proposed a method that can be used to support design decisions and to shorten the overall development process of SCR systems [18].

Gas flow analysis using 1D–3D coupling is a method that can be calculated in 1D or 3D zones depending on the modeled components and is a method that can be quickly calculated by obtaining accurate analysis results [19]. In this study, we proposed a method to analyze intake/exhaust gas flow of a CI engine by coupling 1D and 3D in the valve system.

Marine CI engines are designed in consideration of the pulsating flow of intake/exhaust gas, and when the emission control device is additionally installed in the existing engine, it is necessary to analyze pulsating flow to predict their performance. The pulsating flow is in the form of a pressure wave that is affected by the shape of the exhaust system and the

length of the exhaust pipe, and changes according to the specifications of the engine and the conditions of the intake/exhaust system [20]. In this study, 1D–3D coupling algorithm of the valve system that can analyze pulsation flow was developed using the method of characteristics (MOC), and the gas flow of the CI engine was analyzed using this algorithm. The zone before the exhaust valve was analyzed in 1D and the zone after the exhaust valve was analyzed in 3D, and the results were compared with the experimental results for validation. The reason for 1D–3D coupling applied to the exhaust valve system was to shorten the computation time by 1D approaching the cylinder zone, which took a long time to compute. In addition, since the exhaust system after the exhaust valve was a 3D approach, detailed observation was possible by expressing the gas flow according to the shape of the exhaust port and exhaust pipe as contours. It was expected that the developed 1D–3D coupling algorithm of the valve system can be used for performance prediction and shortens the design process when the emission control device was installed in the CI engine.

2. Theoretical Interpretation

2.1. Method of Characteristics (MOC)

The MOC is a technique for solving first-order partial differential equations by converting it into first-order ordinary differential equations, and a method of calculating the pressure wave in both directions is used to calculate the compressible flow [21]. Benson et al. applied the MOC to the boundary condition of a diesel engine by calculating the pressure wave using Riemann variables called characteristics [22]. It has been verified for accuracy and is used for gas flow analysis of diesel engines [23]. The characteristics can be calculated using a non-dimensional physical quantity and are expressed as λ or β depending on the direction of the pressure wave.

$$\begin{cases} \lambda = A + \frac{\kappa-1}{2} \times U \\ \beta = A - \frac{\kappa-1}{2} \times U \end{cases} \quad (1)$$

where A is the non-dimensional speed of sound, U is the non-dimensional velocity, and the gas flow of the intake/exhaust system of the CI engine is analyzed using λ and β , which are characteristics.

2.2. Gas Flow Thought the Valve

The method of obtaining the characteristics differs depending on whether the condition of the gas flow through the valve is sonic or subsonic [22]. Equation (2) is a pressure function for the boundary of the speed of sound that distinguishes the sonic or the subsonic, and Mach number 1 is in critical conditions.

$$\pi_{\text{critical}} = S_{\kappa} - \frac{\kappa-1}{2} \times \frac{1}{C} \times y, \quad (2)$$

where C is entropy change, S_{κ} is Equation (3) related to the specific heat ratio κ , and is also used to calculate y and C_s .

$$S_{\kappa} = \sqrt{\frac{2}{\kappa+1}}, \quad (3)$$

y is Equation (4) related to the enlarged ratio of the valve opening area ψ , and is the ratio of the area before and after passing through the valve.

$$y = S_{\kappa} \times \frac{\sqrt{1 + (\kappa^2 - 1) \times \psi^2 - 1}}{\psi \times (\kappa - 1)}, \quad (4)$$

C_s is the entropy change when the gas in the cylinder passes through the valve, and is expressed by Equation (5) related to y and S_κ .

$$C_s = \sqrt{1 - \frac{y^2 \times (\kappa - 1)}{2}} \times \frac{1}{S_\kappa}, \quad (5)$$

The gas flow through the valve can be expressed by the pressure function of the valve π_{valve} using the characteristics λ_{inflow} , which can be obtained through the cylinder pressure.

$$\pi_{\text{valve}} = \frac{\lambda_{\text{inflow}}}{\left(\frac{p_{\text{cyl}}}{p_{\text{ref}}}\right)^{\frac{\kappa-1}{2\kappa}}}. \quad (6)$$

π_{valve} is used to check the direction of the gas flow and the condition of the speed of sound. If π_{valve} is greater than 1, the gas flow enters through the valve, and conversely, if it is less than 1, the gas flow exits through the valve. When it is 1, the gas flow does not flow in a state where the pressures of the cylinder and the valve are in equilibrium. In addition, it can be checked whether the gas flow passing through the valve is in a sonic or subsonic condition by comparing it with the π_{critical} in a pressure function for the boundary of the speed of sound in Equation (2). If the π_{valve} is larger than π_{critical} , it is subsonic, and if it is small, it is sonic.

3. 1D–3D Coupling Methodology

Commercial CFD code Ansys Fluent R15.0 was used to analyze intake/exhaust gas flow of the CI engine, and 1D gas flow was calculated using user-defined functions (UDFs) coded using MOC. The 1D and 3D zones were calculated simultaneously and the equations were coded as an open source that could be freely modified so that the correlation between the calculation process and the calculation result could be checked. The 1D–3D coupling algorithm was calculated by the MOC and was coded in C language and applied to the UDFs.

3.1. Modeling

Figure 1 shows the schematic diagram of modeling the experimental apparatus composed of the 4-stroke medium-speed CI engine, and the gas flow was analyzed for the intake/exhaust pipe, ports, valves and the cylinder. The 1D–3D coupling algorithm of the valve system was applied to the exhaust valve, and the experiment and gas flow were analyzed only for the single cylinder in order to minimize the factors affecting the analysis results of the gas flow. In order to verify the accuracy of the 1D–3D coupling for the gas flow through the valve, the combustion reaction was excluded, and the intake/exhaust gas flow pressure in the cold flow state was measured with the experimental apparatus by rotating the flywheel using an electric motor.

Table 1 presents specifications of the experimental apparatus and conditions of the gas flow analysis. If the motion of the piston in the cylinder and the intake/exhaust valves is 3D-modeled, the dynamic mesh must be used to model the same as the actual diesel engine operation, which is a very time-consuming method. To shorten the computation time, the cylinder and intake system were modeled in 1D, and the exhaust port in the shape of a bent and tapered pipe was modeled in 3D. Since a lot of meshes were required to model the long exhaust pipe (1.0 m) in 3D, the part after the pressure measurement position in the exhaust pipe was modeled in 1D in order to quickly calculate it by reducing the number of meshes.

The 1D–3D coupling was applied in two positions, the exhaust valve and the exhaust pipe. The 1D–3D coupling position in the exhaust pipe was 0.15 m away from the cylinder head, and it was the position where the pressure of the exhaust pipe was measured in the experiment. The 1D–3D coupling on the exhaust pipe used the coupling algorithm in the pipe, which was developed in the author's previous research [24]. The 1D–3D coupling

algorithm of the pipe system is a method of calculating the characteristics that contact at the coupling face using linear interpolation, and it is a technique that can be accurately calculated in the straight pipe with an error of 2.20% or less.

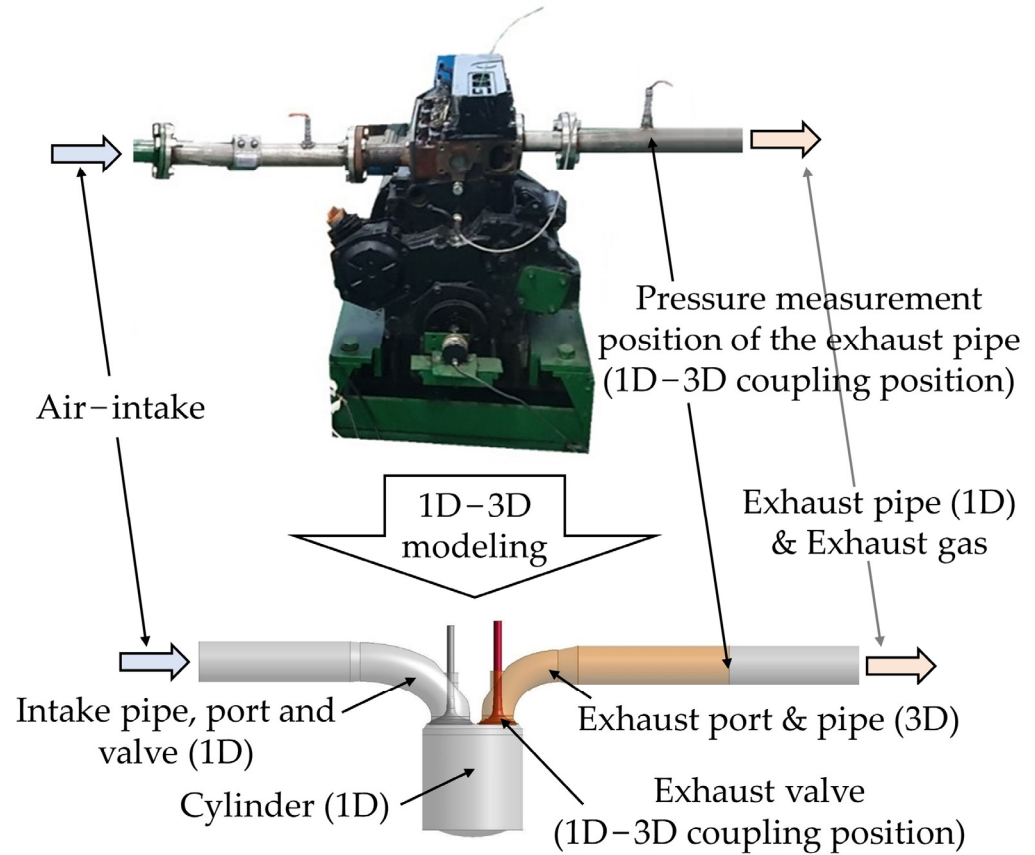


Figure 1. Schematic diagram of modeling the experimental apparatus.

Table 1. Specifications of the experimental apparatus.

Parameters	Values	Unit
Engine speed	700, 900, 1100	RPM
Intake air method	Naturally aspirated (include surge tank)	-
Exhaust outlet boundary condition	Atmosphere	-
Exhaust valve opens (EVO)	130 (before BDC 50)	CA° ¹
Exhaust valve closes (EVC)	378 (after TDC 18)	CA°
Length of exhaust pipe	1.0	m
Diameter of exhaust pipe	0.04	m

¹ CA° refers to the crank angle degrees.

Figure 2 shows the interior face, mesh modeling and position diagrams of the 3D zone required to calculate the 1D-3D coupling algorithm. The interior face was in the 3D zone, and it was generated in the position spaced apart by the mesh size of the 1D zone based on the 1D-3D coupling face. The reason for generating the interior face was that pressure and velocity at the positions of the previous and next meshes were required to obtain characteristics of the 1D-3D coupling face. The position diagram consisting of distance and time step was constructed using the mesh of 1D zone, 1D-3D coupling face, and interior face, and it was calculated using the MOC.

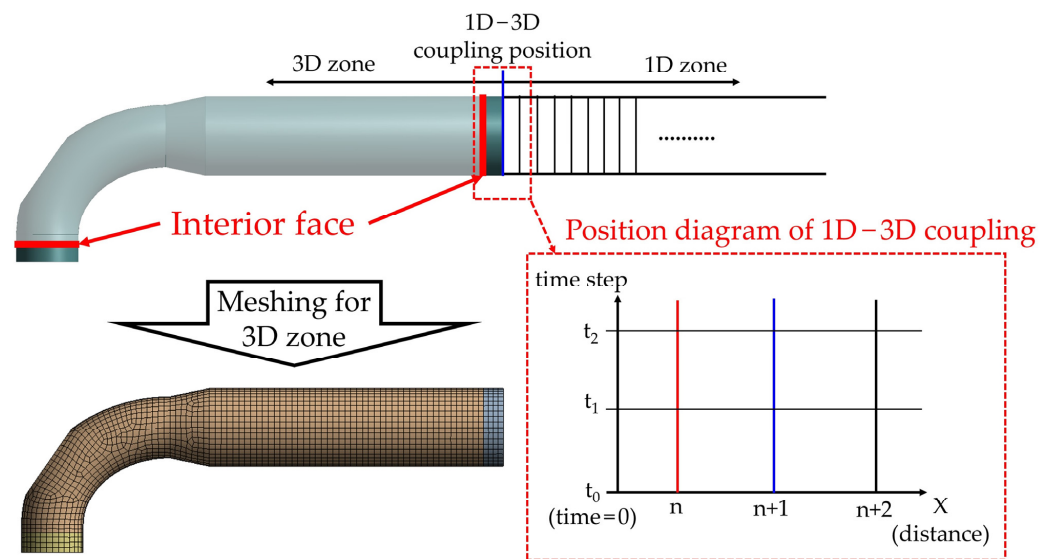


Figure 2. The interior face, mesh modeling and position diagrams used in the 1D–3D coupling algorithm.

3.2. 1D–3D Coupling Algorithm for the Valve System

To calculate the gas flow of the CI engine, the exhaust process of the cylinder was calculated using the exhaust subroutine of the 1D zone. The exhaust subroutine was composed of the valve and nozzle subroutine according to the direction of gas flow through the valve, and when the valve was closed, there was no gas flow through the valve, thus ending the exhaust subroutine. When the valve was opened, the gas flow was calculated using Equation (6) as a function of the pressure of the exhaust valve.

The 1D–3D coupling algorithm of the exhaust valve was the method of calculating using the characteristics of the 1D and 3D zones in the exhaust valve, which was the boundary condition between the cylinder and the exhaust port. Figure 3 shows the flow chart of the 1D–3D coupling algorithm used to analyze the gas flow in the exhaust valve boundary condition. It was the process of calculating the characteristics λ and β that proceed in both directions using the initial value, and then calculating it using the physical quantity at the 1D–3D coupling position and the interior face.

The PROFILE functions of UDFs were used to transfer data from the 1D zone to the 3D zone, and the ADJUST functions were used to calculate the position diagram of the 1D–3D coupling and the exhaust subroutine. The valve subroutine was calculated using the characteristics λ_{inflow} of the 3D zone, and $\lambda_{outflow}$ could be obtained as a result, and the pressure and velocity results could be obtained from the exhaust valve using λ_{inflow} and $\lambda_{outflow}$. The pressure and velocity results obtained through this process were transmitted to the 1D and 3D zones according to the time step to continue the calculation in each zone.

Since the gas flow was analyzed by modeling the exhaust port in the 3D zone, the boundary conditions change depending on the gas flow direction through the exhaust valve. The gas flow entering the cylinder through the exhaust valve was an outlet boundary condition in the 3D zone, but the gas flow exiting the cylinder was an inlet boundary condition in the 3D zone. Therefore, it was necessary to analyze the gas flow by changing the boundary conditions of the 3D zone according to the gas flow direction.

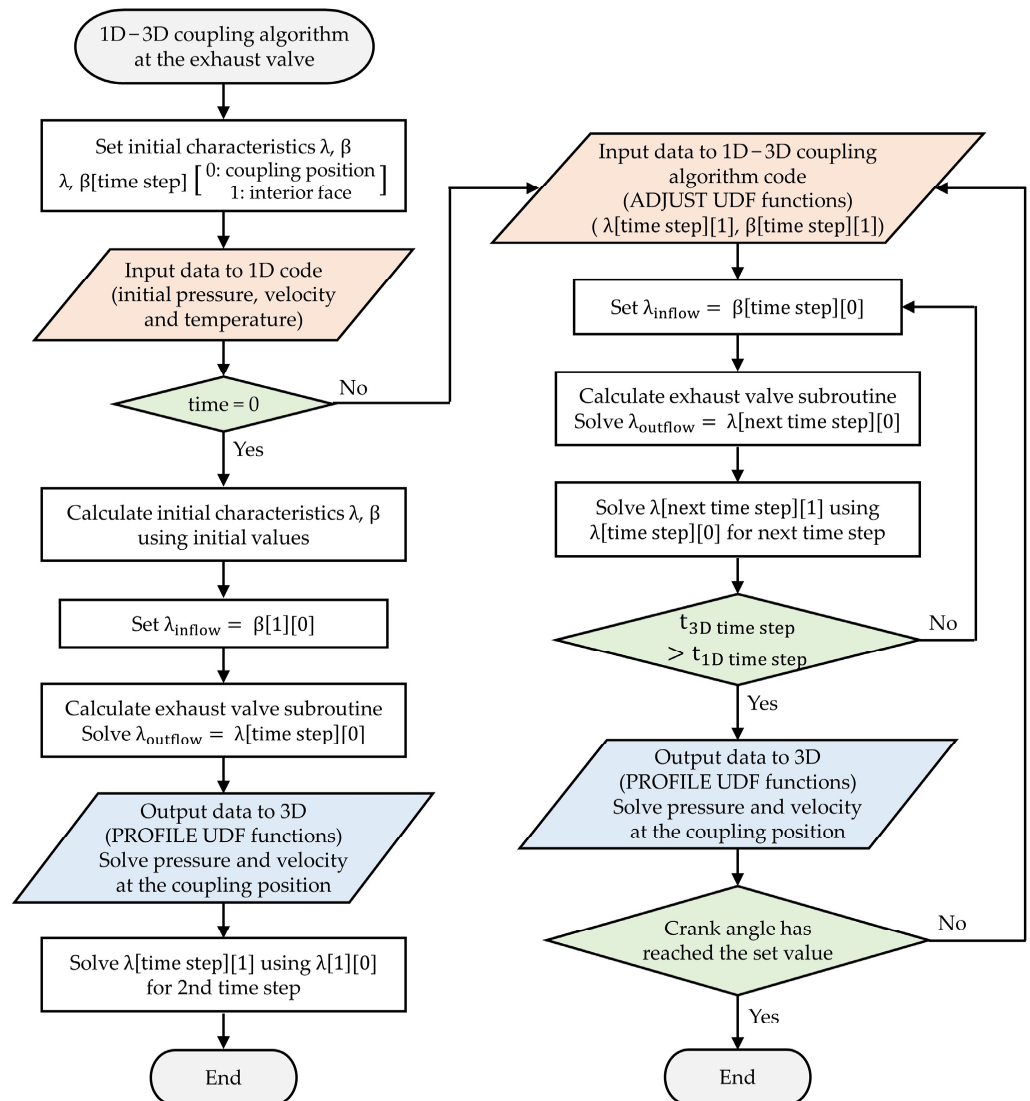


Figure 3. Flow chart of the 1D–3D coupling algorithm in the exhaust valve boundary condition.

4. Validation and Results

Figure 4 shows the cylinder pressure results in the process of opening the exhaust valve and compares the results of the gas flow analysis using the 1D–3D coupling algorithm based on the experimental results. With the gas in the cylinder being exchanged, the piston moves downward until bottom dead center (BDC) 180 CA° and the pressure decreases, and after BDC, the piston moves upward, resulting in an increase in pressure.

The exhaust valve was fully opened at 254 CA°, and a momentary peak occurred because the pressure increased due to the piston moving upward was higher than the pressure decrease due to the gas flow exiting the exhaust valve. Table 2 presents the cylinder pressure at these peaks, and Table 3 presents the timing of the peak after BDC. The cylinder pressure error was within 8.2%, and the timing difference was within 4 CA° at the peak. The cylinder pressure was lower in the gas flow analysis results than in the experimental results, and the timing of the peaks appeared late. Since these results appeared at the same at all engine speeds, it was expected that this could be calibrated by a correction method that applies the flow coefficient passing through the valve in the future.

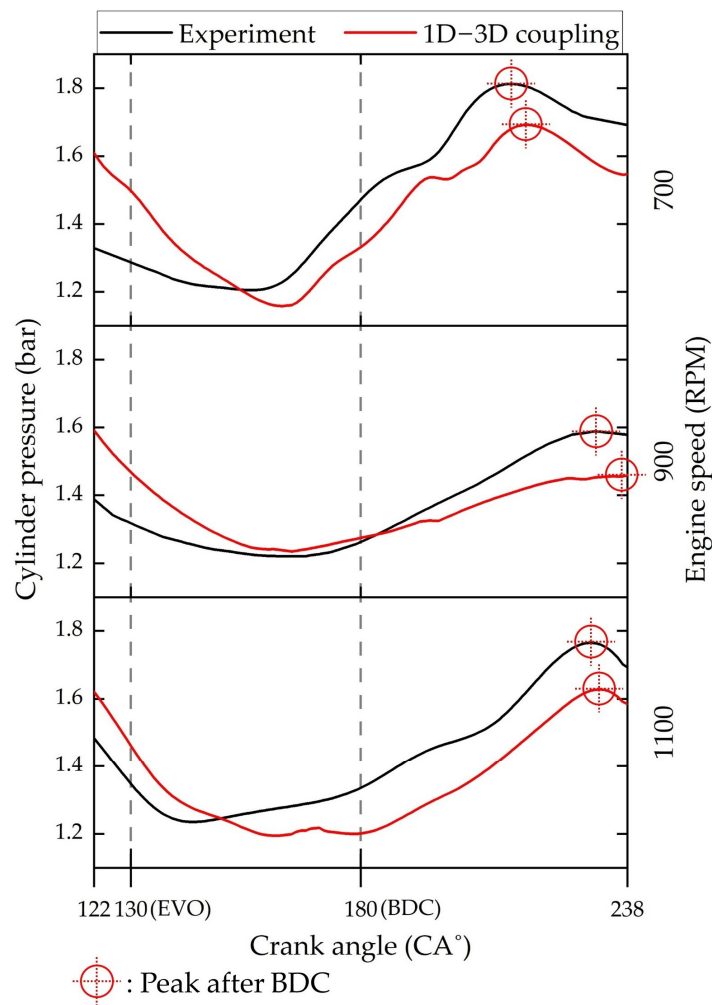


Figure 4. Cylinder pressure results in the process of opening the exhaust valve.

Table 2. Cylinder pressure results at the peak according to the engine speed.

Engine Speed (RPM)	Cylinder Pressure at the Peak (bar)		Error (%)
	Experimental	1D-3D Coupling	
700	1.81	1.69	6.6
900	1.59	1.46	8.2
1100	1.77	1.63	7.9

Table 3. Timing of the peak after BDC according to the engine speed.

Engine Speed (RPM)	Timing of the Peak After BDC (CA°)		Error (CA°)
	Experimental	1D-3D Coupling	
700	213	216	3
900	232	236	4
1100	230	232	2

Figure 5a shows a comparison of the exhaust pipe pressure from the exhaust process to the BDC (540 CA°) with the results of the 1D-3D coupling gas flow analysis based on the experimental results. The direction in which the exhaust valve was located in the exhaust pipe was determined by the boundary condition depending on the open/closed state of the valve, and the opposite direction where the gas flow was discharged to the atmosphere was the open-end boundary condition, where the gas flow exited and was affected by

the reflected wave. During the exhaust process, the pressure of the exhaust pipe did not appear in a periodic form due to the influence of the gas flow out of the cylinder, but the pressure in the exhaust pipe appeared in a periodic form after the exhaust valve was closed at 378 CA°. After BDC (180 CA°) of the exhaust process, the pressure increased due to the piston moving upward and the maximum exhaust pipe pressure appeared. Table 4 presents a comparison of the maximum exhaust pipe pressure results of the experimental and the gas flow analysis. When comparing the maximum pressure to verify the pressure results of the exhaust pipe based on the experimental result, the error was found to be less than 1.30%. Figure 5b shows an enlarged view of the section after the exhaust valve was closed. The pressure and phase results were different depending on the engine speed, and the pressure wave passing through the exhaust pipe and the reflected wave generated at the open end were overlapping, and the pressure results appeared in the form of a pulsating flow with periodic peaks. Table 5 presents a comparison of the timing of the first peak after BDC, and the experiments and the gas flow analysis results were consistent at 700 and 1100 RPM. At 900 RPM, a difference of 4 CA° occurred in the timing at which the peak appeared, and the difference in pressure was larger than that of other engine speeds. The method of correcting the result by applying the flow coefficient was expected to have to apply a different value depending on the engine speed.

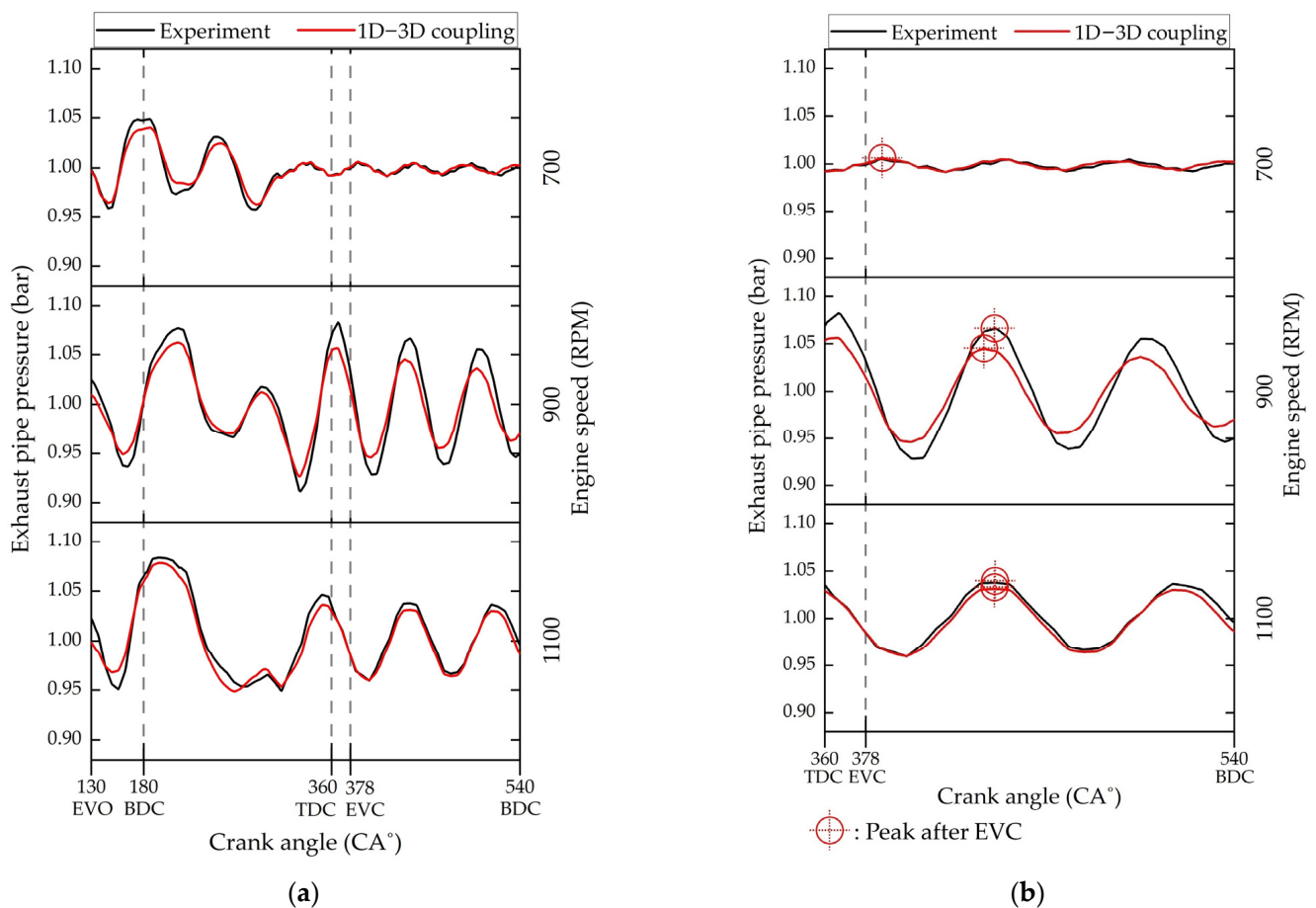


Figure 5. Exhaust pipe pressure results during the exhaust process: (a) From exhaust valve opened to bottom dead center 540 CA°; (b) from top dead center 360 CA° to bottom dead center 540 CA°.

Table 4. Maximum pressure results of the exhaust pipe after BDC according to the engine speed.

Engine Speed (RPM)	Maximum Pressure After BDC (bar)		Error (%)
	Experimental	1D–3D Coupling	
700	1.049	1.039	0.95
900	1.076	1.062	1.30
1100	1.084	1.076	0.74

Table 5. Timing of the peak after EVC according to the engine speed.

Engine Speed (RPM)	Timing of the Peak After EVC (CA°)		Error (CA°)
	Experimental	1D–3D Coupling	
700	385	385	0
900	435	431	4
1100	435	435	0

Figure 6 shows the contour representation of the pressure (a) and velocity (b) results of the gas flow passing through the exhaust port at 254 CA° with the exhaust valve fully opened, and the gas flow in the cylinder in outflow conditions. As the gas flow passed through the bent and tapered pipe of the exhaust port, a section in which the pressure was changed appeared, and a section in which the velocity was increased in the bent pipe appeared.

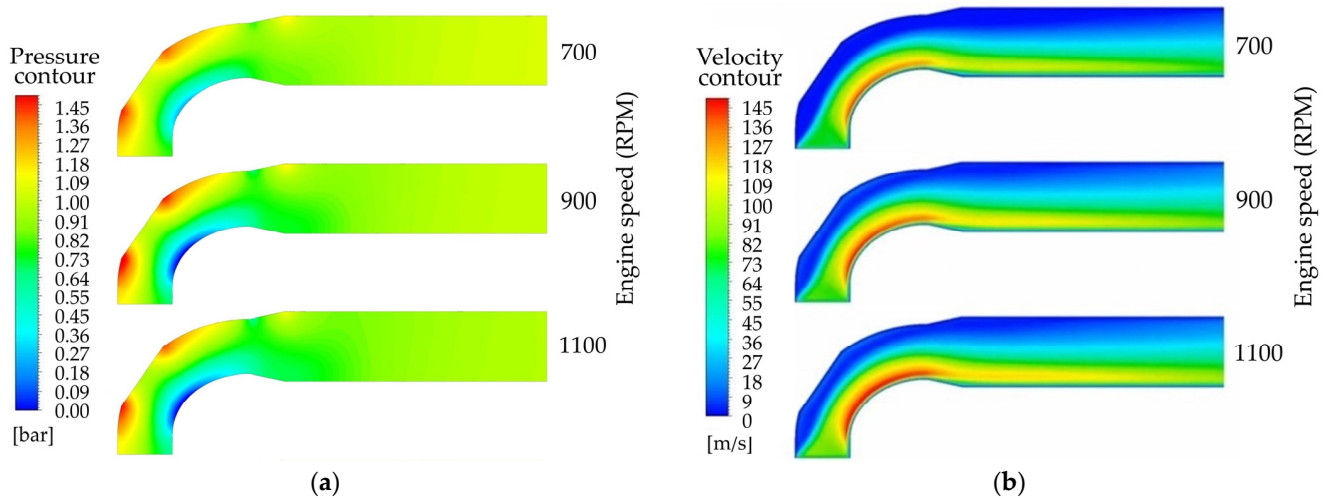


Figure 6. Contour results of exhaust port in the 3D zone at exhaust valve fully opened (254 CA°): (a) Pressure contours; (b) velocity contours.

For complex shapes such as bent and tapered pipes, the 1D gas flow analysis was simplified to a straight pipe, but it could be calculated in 3D using the 1D–3D coupling algorithm. In addition, detailed gas flow could be observed by contouring the pressure and velocity results. By utilizing the 1D–3D coupling algorithm, it was expected to be able to observe the gas flow that changes according to various shapes in detail.

It took about 30 min of computation time to analyze the gas flow of the CI engine in this study (using an 8-core central processing unit). It was computed about 336 times faster, as it took about 7 days to analyze the same CI engine in 3D. The gas flow analysis using the 1D–3D coupling algorithm, which was able to obtain accurate results in a short time, can obtain calculation results within a few hours for various models. This advantage was expected to be highly useful for optimization according to shape.

If the main observation target was an emission control device that was additionally installed in the CI engine, it was necessary to focus on it and lighten the analysis of the

CI engine. The 1D–3D coupling algorithm could be utilized to shorten the development process of these emission control devices. It could be modeled in the 1D or 3D zone according to the user's request, and performance prediction according to shape change could be performed quickly by modeling the exhaust system and manifold in 3D. It was expected that it could be used to analyze the pulsation effect and the ram effect by using the fact that the flow could be expressed as contours in the 3D zone.

5. Conclusions

In order to quickly and accurately calculate the gas flow of the CI engine, the 1D–3D coupling algorithm that could be applied to the valve system was developed. The results of the gas flow analysis using this algorithm were verified by comparing them with the experimental results, as summarized below:

- (1) An algorithm for coupling 1D and 3D for valve systems was developed by applying the calculation using the MOC to a commercial CFD code;
- (2) In the case of analyzing the gas flow using the 1D–3D coupling algorithm, it could be computed within 30 min. This was 336 times faster than calculating the entire system in 3D;
- (3) The results of analyzing the pressure of the exhaust pipe using the 1D–3D coupling algorithm showed that the error was within 1.30% when compared with the experimental results; and
- (4) It was possible to analyze the zone requiring visualization of the flow in 3D and confirm the result according to the shape as contours.

To analyze the intake/exhaust gas flow of the CI engine, the 1D–3D coupling algorithm was used to quickly calculate the accurate results. It was expected that it could be used as an analysis method including the CI engine to predict the performance of emission control devices such as SCR and scrubber. Using the advantage of being able to analyze the gas flow of the entire intake/exhaust system, the follow-up study will analyze the effect of changes in the shape of the intake/exhaust system on the engine. If the design of experiments (DoEs) and 1D–3D coupling approach are used together to optimize the intake/exhaust system, it is expected that it will be utilized to design the shape in consideration of the pulsating flow and the ram effect.

Funding: This research received no external funding.

Institutional Review Board Statement: Not applicable.

Informed Consent Statement: Not applicable.

Data Availability Statement: Not applicable.

Conflicts of Interest: The author declares no conflict of interest.

References

1. Guidelines for Port State Control Under MARPOL Annex VI Chapter 3. 2019. Available online: [https://wwwcdn.imo.org/localresources/en/OurWork/Environment/Documents/MEPC.321\(74\).pdf](https://wwwcdn.imo.org/localresources/en/OurWork/Environment/Documents/MEPC.321(74).pdf) (accessed on 10 September 2021).
2. Winnes, H.; Fridell, E.; Moldanová, J. Effects of marine exhaust gas scrubbers on gas and particle emissions. *J. Mar. Sci. Eng.* **2020**, *8*, 299. [CrossRef]
3. Guidance on the Application of Regulation 13 of MARPOL Annex VI Tier III Requirements to Dual Fuel and Gas-Fuelled Engines. Available online: <https://wwwcdn.imo.org/localresources/en/OurWork/Environment/Documents/MEPC%201-Circ%20854.pdf> (accessed on 10 September 2021).
4. Fan, H.; Tu, H.; Enshaei, H.; Xu, X.; Wei, Y. Comparison of the economic performances of three sulphur oxides emissions abatement solutions for a very large crude carrier (VLCC). *J. Mar. Sci. Eng.* **2021**, *9*, 221. [CrossRef]
5. Wu, P.-C.; Lin, C.-Y. Cost-Benefit Evaluation on promising strategies in compliance with low sulfur policy of IMO. *J. Mar. Sci. Eng.* **2020**, *9*, 3. [CrossRef]
6. Tran, T.A. Some methods to prevent the wear of piston-cylinder when using low sulphur fuel oil (LSFO) for all ships sailing on emission control areas (ECAs). In *Diesel and Gasoline Engines*; Viskup, R., Ed.; IntechOpen: London, UK, 2020; ISBN 978-1-78985-248-6.

7. Technology for Ecology. Available online: https://www.man-es.com/docs/default-source/marine/2366382_technology-forecology_21082020.pdf (accessed on 10 September 2021).
8. Altosole, M.; Balsamo, F.; Campora, U.; Mocerino, L. Marine dual-fuel engines power smart management by hybrid turbocharging systems. *J. Mar. Sci. Eng.* **2021**, *9*, 663. [[CrossRef](#)]
9. Akgül, V.; Özener, O.; Büyük, C.; Özkan, M. Numerical investigation and multi-objective optimization of internal egr and post-injection strategies on the combustion, emission and performance of a single cylinder, heavy-duty diesel engine. *Energies* **2020**, *14*, 15. [[CrossRef](#)]
10. Kim, D.; Lee, C. SCR Performance evaluations in relation to experimental parameters in a marine generator engine. *J. Mar. Sci. Eng.* **2019**, *7*, 67. [[CrossRef](#)]
11. Zhu, Y.; Zhang, R.; Zhou, S.; Huang, C.; Feng, Y.; Shreka, M.; Zhang, C. Performance optimization of high-pressure scr system in a marine diesel engine. Part I: Flow optimization and analysis. *Top. Catal.* **2019**, *62*, 27–39. [[CrossRef](#)]
12. Dimitrakopoulos, N.; Belgiorno, G.; Tuner, M.; Tunestal, P.; Blasio, G.D.; Beatrice, C. PPC Operation with Low RON Gasoline Fuel. A Study on Load Range on a Euro 6 Light Duty Diesel Engine. In Proceedings of the Ninth International Conference on Modeling and Diagnostics for Advanced Engine Systems (COMODIA 2017), Okayama Convention Center, Okayama, Japan, 25–28 July 2017. [[CrossRef](#)]
13. Beatrice, C.; Belgiorno, G.; Di Blasio, G.; Mancaruso, E.; Sequino, L.; Vaglieco, B.M. *Analysis of a Prototype High-Pressure “Hollow Cone Spray” Diesel Injector Performance in Optical and Metal Research Engines*; SAE: Warrendale, PA, USA, 2017.
14. Chowdary, P.K.; Ganji, P.R.; Kumar, M.S.; Kumar, C.R.; Rao, S.S. Numerical analysis of C.I engine to control emissions using exhaust gas recirculation and advanced start of injection. *Alex. Eng. J.* **2016**, *55*, 1881–1891. [[CrossRef](#)]
15. Zhu, Y.; Li, T.; Xia, C.; Feng, Y.; Zhou, S. Simulation analysis on vaporizer/mixer performance of the high-pressure SCR system in a marine diesel. *Chem. Eng. Process. Process. Intensif.* **2020**, *148*, 107819. [[CrossRef](#)]
16. De Robbio, R.; Cameretti, M.; Mancaruso, E.; Tuccillo, R.; Vaglieco, B. CFD Study and Experimental Validation of a Dual Fuel Engine: Effect of Engine Speed. *Energies* **2021**, *14*, 4307. [[CrossRef](#)]
17. Liu, Y.; Kuznetsov, A.; Sa, B. Simulation and Analysis of the impact of cylinder deactivation on fuel saving and emissions of a medium-speed high-power diesel engine. *Appl. Sci.* **2021**, *11*, 7603. [[CrossRef](#)]
18. Wurzenberger, J.C.; Wanker, R. Multi-Scale SCR Modeling, 1D Kinetic Analysis and 3D System Simulation. *SAE Trans.* **2005**, *114*, 344–362. [[CrossRef](#)]
19. Kim, K.-H.; Kong, K.-J. 1D–3D Coupling for gas flow analysis of the air-intake system in a compression ignition engine. *J. Mar. Sci. Eng.* **2021**, *9*, 553. [[CrossRef](#)]
20. Eddine, A.N.; Chalet, D.; Faure, X.; Aixala, L.; Chessé, P. Effect of engine exhaust gas pulsations on the performance of a thermoelectric generator for wasted heat recovery: An experimental and analytical investigation. *Energy* **2018**, *162*, 715–727. [[CrossRef](#)]
21. Burnat, M. The method of characteristics and Riemann invariants for multidimensional hyperbolic systems. *Sib. Math. J.* **1970**, *11*, 210–232. [[CrossRef](#)]
22. Winterbone, D.E.; Pearson, R.J. *Theory of Engine Manifold Design: Wave Action Methods for IC Engines*; Wiley-Blackwell: Hoboken, NJ, USA, 2000.
23. Kim, K.-H.; Kong, K.-J. One-Dimensional gas flow analysis of the intake and exhaust system of a single cylinder diesel engine. *J. Mar. Sci. Eng.* **2020**, *8*, 1036. [[CrossRef](#)]
24. Kong, K.-J.; Jung, S.-H.; Jeong, T.-Y.; Koh, D.-K. 1D-3D coupling algorithm for unsteady gas flow analysis in pipe systems. *J. Mech. Sci. Technol.* **2019**, *33*, 4521–4528. [[CrossRef](#)]